Cyclic OFF/Part/ON switching of single-molecule magnet behaviours via multistep single-crystal-to-single-crystal transformation between discrete Fe(II)-Dy(III) complexes

Wen-Bin Chen,[ab] Yan-Cong Chen,*[a] Guo-Zhang Huang,[a] Jun-Liang Liu,[a] Jian-Hua Jia*[a] and Ming-Liang Tong*[a]

[a] MOE Key Lab of Bioinorganic and Synthetic Chemistry, School of Chemistry, Sun Yat-Sen University, Guangzhou 510275, P. R. China.

[b] School of Chemistry and Chemical Engineering, Guangzhou University, Guangzhou 510006, P. R. China.

EXPERIMENTAL SECTION

Materials and Physical Measurements. All reagents were commercially available and used as received without further purification. The ligand of methyl-2-pyridyl ketone oxime (mepaoH) was synthesized according to the method reported in reference.[1] The C, H, N and S elemental analyses were carried out with an Elementar Vario-EL CHNS elemental analyzer. IR spectra were recorded using pressed KBr pellets on a Thermo Scientific Nicolet 6700-Contiuμm spectrometer. X-ray powder diffraction (XRPD) performed on polycrystalline samples were measured on Bruker D8 Advance Diffractometer (Cu-K_α, λ = 1.54056 Å). Simulated patterns were generated with Mercury. Thermogravimetric analyses (TGA) were carried out on a NETZSCH TG209F3 thermogravimetric analyzer. Magnetic susceptibility measurements were performed with a Quantum Design MPMS-XL7 SQUID. Polycrystalline samples were embedded in vaseline to prevent torqueing. Data were corrected for the diamagnetic contribution calculated from Pascal constants. The ambient humidity is measured with a hygrometer.

Single Crystal X-ray Crystallography. Single-crystal X-ray diffraction studies were performed at various temperatures on a Bruker D8 QUEST diffractometer equipped with Mo-K_α

(λ = 0.71073 Å) high-brilliance IμS (micro-source) radiation and a PHOTON 100 CMOS detector. The instrument was controlled with the APEX3 software package. The crystal data of **1-3** were collected with same single crystal. Multi-scan absorption correction was performed using SADABS-2014/5. The structures were solved using intrinsic phasing methods (SHELXT) supplied within the APEX3 suite. Using OLEX2, data were refined by full-matrix least-squares using SHELXL (2018/1) program packages.[2, 3] Anisotropic thermal parameters were applied to all non-hydrogen atoms. Hydrogen atoms were located from difference maps and refined with isotropic temperature factors. In complex **1**, the atoms S2, S3, C30, C31, N10 and N11 of SCN counter anion are each disordered over two positions and refined with an assigned site-occupancy ratio of 0.5:0.5, respectively. The O3w, O4w, O5w and O6w of lattice water molecule occupied same coordinates with S2, S3, N10 and N11, respectively. The site-occupancy ratios of them are 0.5. The H atoms of lattice water molecule were not added because of the disorder. For complex **2** and **3**, the structure contains solvent accessible voids of 186 and 162 Å^3, respectively. Thus, the crystal data were refined using the SQUEEZE procedure from the PLATON software.[4] Crystallographic Data Centre under reference numbers CCDC 1837942-1837944 for **1-3** contain the supplementary crystallographic data for this paper. These data can be obtained free of charge via www.ccdc.cam.ac.uk/conts/retrieving.html (or from the Cambridge Crystallographic Data Centre, 12 Union Road, Cambridge CB21EZ, UK; fax: (+44)1223-336-033; or deposit@ccdc.cam.ac.uk).

Synthesis of [FeDy(mepao)$_3$(mepaoH)(NCS)(H$_2$O)$_2$](SCN)·2H$_2$O (1). A mixture of $FeSO_4$ (0.014g, 0.05 mmol), $Dy(acac)_3(H_2O)_2$ (0.025 g, 0.05 mmol), NH_4SCN (0.08 g, 0.1 mmol)and mepaoH (0.030 g, 0.2 mmol), in 15 mL of MeOH was heated in a stainless steel reactor with 25 mL sealed Teflon liner at 348 K for 12 h and then cooled to room temperature at a rate of 5 K/h. The resultant mixture was filtered and deep red block crystals were obtained by slow evaporation of the filtrate after several days. The deep red block crystals were washed with ethanol and dried in air. Yield: 59.2% for **1** based on Dy^{3+}. Elemental Anal. Calcd for **1** of $C_{30}H_{37}DyFeN_{10}O_8S_2$ (%): C, 38.00; H, 3.93; N, 14.77; S,6.76; Found(%): C, 37.89; H, 3.69; N, 14.93; S,6.45. FT-IR (KBr, cm^{-1}): 3052 (s), 2062 (s), 1630 (m), 1597 (s), 1570 (m), 1525 (m), 1464 (s), 1433 (s), 1373 (m),

1346 (m),1288 (w), 1251 (w), 1157 (s), 1101 (s), 1076 (s), 1043 (s), 1057 (m), 1012 (s), 971 (m), 813 (m), 773 (s), 746 (m), 692 (s), 631(w), 534 (w), 505 (m), 459 (m).

Synthesis of $[FeDy(mepao)_3(mepaoH)(NCS)_2(H_2O)]\cdot 2H_2O$ (2). Crystals of **1** were heated from 120 K to 298 K with a rate of 6 K/min, and then the temperature was kept constant for 30 min in the Bruker D8 QUEST diffractometer. Then, crystals of **2** can be obtained. Large numbers of samples **2** were obtained via keeping the samples of **1** in 308 K for 30 minute at TG. Elemental Anal. Calcd for **2** of $C_{30}H_{35}DyFeN_{10}O_7S_2$ (%): C, 38.74; H, 3.79; N, 15.06; S,6.89; Found(%): C, 38.98; H, 3.71; N, 15.29; S,6.90. FT-IR (KBr, cm^{-1}): 3052 (s), 2062 (s), 1631 (m), 1597 (s), 1568 (m), 1525 (m), 1464 (s), 1433 (s), 1375 (m), 1346 (m),1288 (w), 1251 (w), 1157 (s), 1101 (s), 1076 (s), 1043 (s), 1057 (m), 1012 (s), 972 (m), 814 (m), 773 (s), 746 (m), 692 (s), 631(w), 532 (w), 505 (m), 462 (m).

Synthesis of $[Fe_2Dy_2(mepao)_6(mepaoH)_2(NCS)_4]$ (3). Crystals of **2** were heated from 298 K to 373 K with a rate of 6 K/min, and then the temperature was kept constant for 10 min in the Bruker D8 QUEST diffractometer. Then, crystals of **3** can be obtained. The crystal data of **3** was collected in 120 K due to weak diffraction in the high temperature (373 K). Large numbers of samples **3** were obtained via keeping the samples of **1** in 373 K for 30 minute at TG. Elemental Anal. Calcd for **3** of $C_{60}H_{58}Dy_2Fe_2N_{20}O_8S_4$ (%): C, 41.13; H, 3.34; N, 15.99; S,7.32; Found(%): C, 41.09; H, 3.37; N, 15.92; S,7.21. FT-IR (KBr, cm^{-1}): 3052 (s), 2062 (s), 1632 (w), 1597 (s), 1568 (m), 1525 (m), 1464 (s), 1433 (s), 1375 (m), 1346 (m),1288 (w), 1252 (w), 1157 (s), 1103 (s), 1076 (s), 1045 (s), 1057 (m), 1012 (s), 975 (m), 814 (m), 773 (s), 748 (m), 694 (s), 605(w), 532 (w), 507 (m), 474 (m).

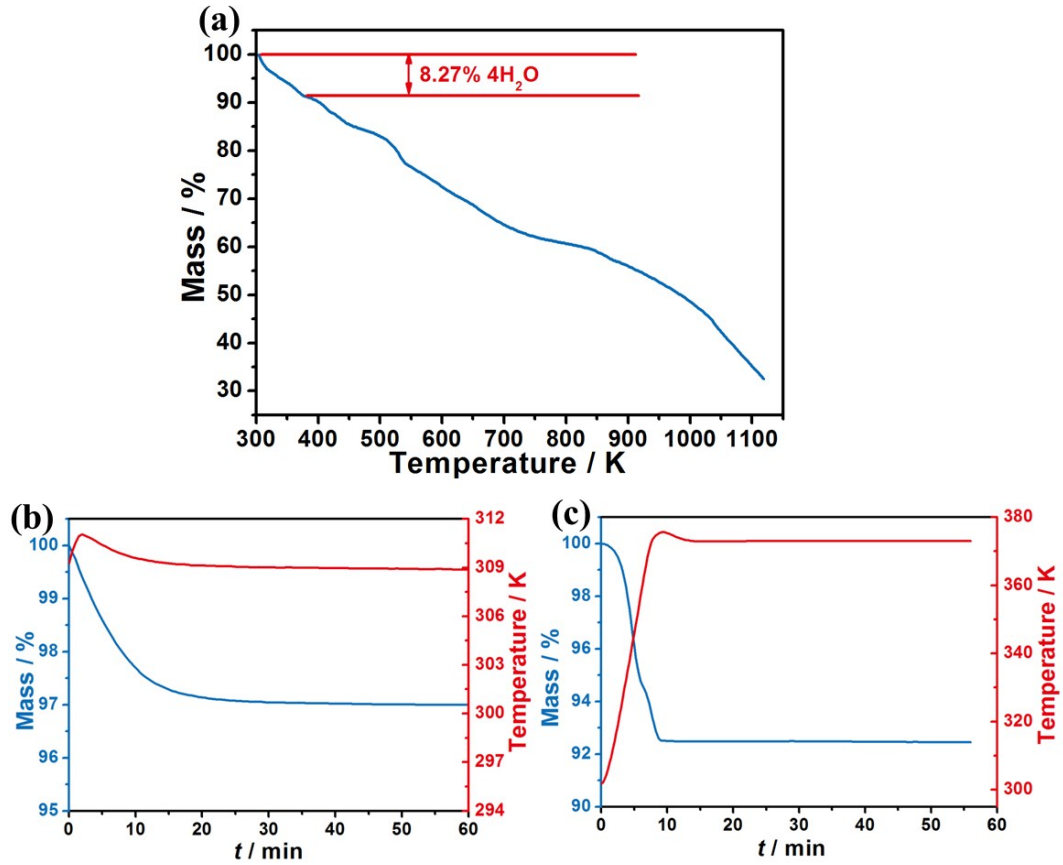

Fig. S1. Temperature-dependent thermogravimetric analysis (TGA) (a), time-dependent TGA at 308 K(b) and 373 K(c) of **1**.

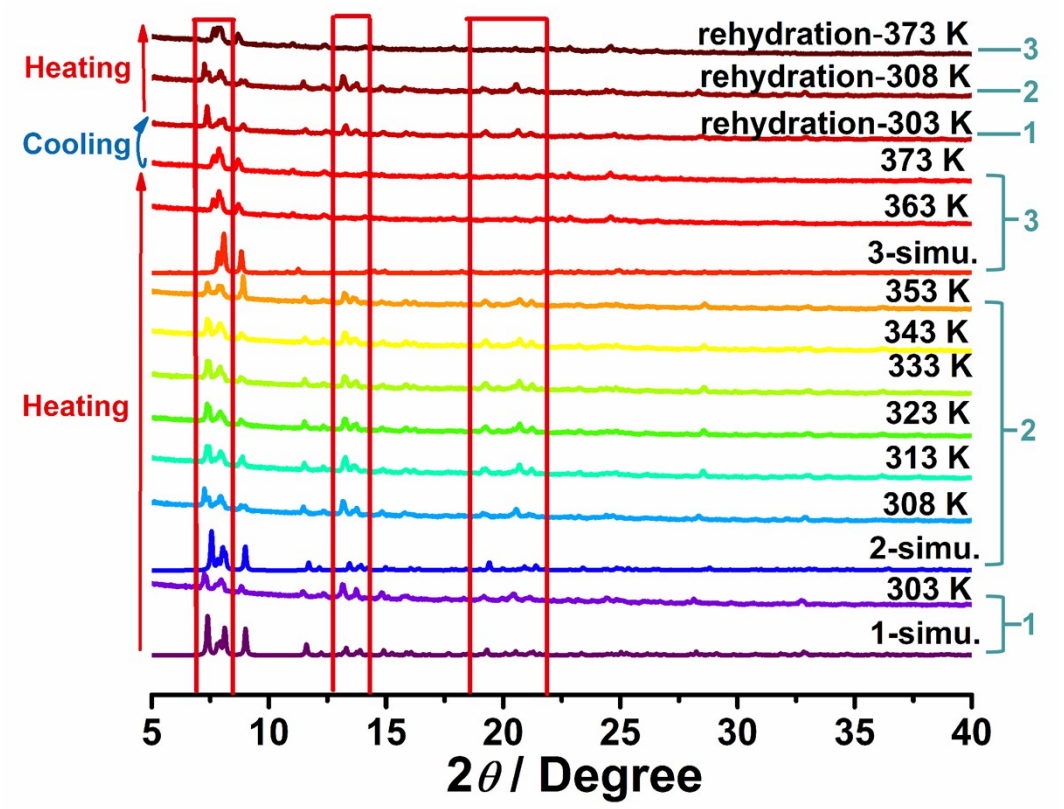

Fig. S2. Variable temperature powder X-ray diffraction patterns. When complex **1** was heated from 303 K to 373 K, it would transform into **2** at 308 K and then **3** after 363 K. When complex **3** was cooled from 373 K to 303 K, **1** was reobtained by rehydration. By heating again, complexes **2** and **3** could be obtained at 308 K and 373 K, respectively. The diffraction patterns are identical to their simulated ones.

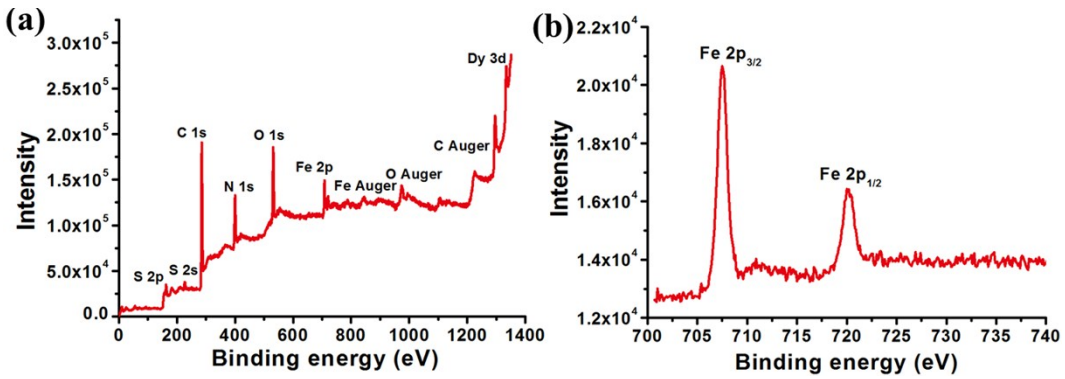

Fig. S3. (a) XPS of 0-1400 eV (b) XPS of 700-740 eV for complex **1**.

Table S1. Crystal data and structure refinement for **1-3**.

Complex	**1**	**2**	**3**
Empirical formula	$C_{30}H_{37}DyFeN_{10}O_8S_2$	$C_{30}H_{35}DyFeN_{10}O_7S_2$	$C_{60}H_{58}Dy_2Fe_2N_{20}O_8S_4$
Formula weight	948.13	930.15	1752.20
Temperature/K	120.0	298	120.0
Crystal system	triclinic	triclinic	triclinic
Space group	*P*-1	*P*-1	*P*-1
a / Å	12.5138(5)	12.617(4)	14.4632(12)
b / Å	13.4439(6)	13.314(3)	15.3659(13)
c / Å	13.7508(6)	13.742(4)	15.8216(13)
α /°	111.4050(10)	111.140(8)	89.095(3)
β /°	112.6130(10)	112.417(8)	83.157(3)
γ /°	98.3890(10)	98.797(8)	85.417(3)
Volume/Å^3	1874.72(14)	1874.0(9)	3479.9(5)
Z	2	2	2
ρ_{calc}(g/cm^3)	1.680	1.648	1.672
μ/mm^{-1}	2.537	2.534	2.718
F(000)	9450	930	1740.0
Reflections collected	42169	34789	62874
Independent reflections	8156 [R_{int}= 0.0286]	8512 [R_{int}= 0.0780]	14276 [R_{int}= 0.0634]
Data/restraints/parameters	8156/12/484	8512/6/447	14276/3/875
Goodness-of-fit on F^2	1.140	1.056	1.192
Final R indexes [I>=2σ (I)]	R_1= 0.0376, wR_2= 0.1022	R_1= 0.0880, wR_2= 0.2430	R_1= 0.0772, wR_2= 0.1510
Final R indexes [all data]	R_1= 0.0420, wR_2= 0.1046	R_1= 0.1238, wR_2= 0.2776	R_1= 0.1250, wR_2= 0.1824
Largest diff. peak/hole / e Å^{-3}	2.98/-2.42	3.31/-2.52	4.34/-2.23
CCDC	1837942	1837943	1837944

[a] $R_1 = \sum||F_o|-|F_c||/\sum|F_o|$. [b] $wR_2 = [\sum w(F_o^2 - F_c^2)^2/\sum w(F_o^2)^2]^{1/2}$

Table S2. Selected bonds lengths [Å] and angles [°] for **1**.

1			
Dy(1)-O(1)	2.352(3)	Dy(1)-O(2W)	2.407(4)
Dy(1)-O(3)	2.313(3)	Dy(1)-N(7)	2.574(4)
Dy(1)-O(2)	2.321(3)	Dy(1)-N(8)	2.497(4)
Dy(1)-O(1W)	2.408(3)	Dy(1)-N(9)	2.438(4)
Fe(1)-N(1)	1.965(4)	Fe(1)-N(4)	1.911(4)
Fe(1)-N(2)	1.908(4)	Fe(1)-N(5)	1.970(4)
Fe(1)-N(3)	1.972(4)	Fe(1)-N(6)	1.916(4)
O(1)-Dy(1)-O(1W)	121.12(11)	O(2W)-Dy(1)-N(7)	77.68(13)
O(1)-Dy(1)-O(2W)	73.16(12)	O(2W)-Dy(1)-N(8)	72.70(14)
O(1)-Dy(1)-N(7)	129.87(11)	O(2W)-Dy(1)-N(9)	136.98(14)
O(1)-Dy(1)-N(8)	71.15(12)	N(8)-Dy(1)-N(7)	61.59(12)
O(1)-Dy(1)-N(9)	149.61(12)	N(9)-Dy(1)-N(7)	72.10(13)
O(3)-Dy(1)-O(1)	80.39(11)	N(9)-Dy(1)-N(8)	115.93(13)
O(3)-Dy(1)-O(2)	86.74(11)	N(1)-Fe(1)-N(3)	94.06(16)
O(3)-Dy(1)-O(1W)	146.18(12)	N(1)-Fe(1)-N(5)	96.03(16)
O(3)-Dy(1)-O(2W)	141.51(13)	N(2)-Fe(1)-N(1)	81.03(16)
O(3)-Dy(1)-N(7)	99.67(12)	N(2)-Fe(1)-N(3)	95.62(16)
O(3)-Dy(1)-N(8)	72.55(12)	N(2)-Fe(1)-N(4)	91.02(16)
O(3)-Dy(1)-N(9)	74.55(12)	N(2)-Fe(1)-N(5)	170.21(17)
O(2)-Dy(1)-O(1)	79.84(11)	N(2)-Fe(1)-N(6)	90.20(16)
O(2)-Dy(1)-O(1W)	73.46(11)	N(4)-Fe(1)-N(1)	170.28(16)
O(2)-Dy(1)-O(2W)	114.75(13)	N(4)-Fe(1)-N(3)	81.09(16)
O(2)-Dy(1)-N(7)	150.17(12)	N(4)-Fe(1)-N(5)	92.72(16)
O(2)-Dy(1)-N(8)	146.55(12)	N(4)-Fe(1)-N(6)	92.53(15)
O(2)-Dy(1)-N(9)	81.82(12)	N(5)-Fe(1)-N(3)	93.90(18)
O(1W)-Dy(1)-N(7)	86.02(12)	N(6)-Fe(1)-N(1)	93.08(15)
O(1W)-Dy(1)-N(8)	136.35(13)	N(6)-Fe(1)-N(3)	171.42(16)
O(1W)-Dy(1)-N(9)	75.68(13)	N(6)-Fe(1)-N(5)	80.60(17)
O(2W)-Dy(1)-O(1W)	72.31(14)		

Table S3. Selected bonds lengths [Å] and angles [°] for **2**.

2			
Dy(1)-O(1)	2.346(8)	Dy(1)-N(7)	2.594(10)
Dy(1)-O(1W)	2.415(9)	Dy(1)-N(8)	2.500(10)
Dy(1)-O(3)	2.306(9)	Dy(1)-N(9)	2.461(10)
Dy(1)-O(2)	2.321(7)	Dy(1)-N(10)	2.450(14)
Fe(1)-N(1)	1.977(9)	Fe(1)-N(4)	1.908(10)
Fe(1)-N(2)	1.905(10)	Fe(1)-N(5)	1.972(11)
Fe(1)-N(3)	1.965(10)	Fe(1)-N(6)	1.941(9)
O(1)-Dy(1)-O(1W)	119.0(3)	N(8)-Dy(1)-N(7)	61.9(3)
O(1)-Dy(1)-N(7)	131.1(3)	N(9)-Dy(1)-N(7)	71.3(4)
O(1)-Dy(1)-N(8)	71.4(3)	N(9)-Dy(1)-N(8)	116.8(4)
O(1)-Dy(1)-N(9)	149.2(3)	N(10)-Dy(1)-N(7)	76.0(4)
O(1)-Dy(1)-N(10)	79.0(4)	N(10)-Dy(1)-N(8)	75.0(5)
O(1W)-Dy(1)-N(7)	90.4(3)	N(10)-Dy(1)-N(9)	131.4(4)
O(1W)-Dy(1)-N(8)	139.7(3)	N(2)-Fe(1)-N(1)	80.4(4)
O(1W)-Dy(1)-N(9)	75.3(4)	N(2)-Fe(1)-N(3)	94.8(4)
O(1W)-Dy(1)-N(10)	69.9(4)	N(2)-Fe(1)-N(4)	91.5(4)
O(3)-Dy(1)-O(1)	80.3(3)	N(2)-Fe(1)-N(5)	170.6(5)
O(3)-Dy(1)-O(1W)	144.5(3)	N(2)-Fe(1)-N(6)	91.0(4)
O(3)-Dy(1)-O(2)	86.0(3)	N(3)-Fe(1)-N(1)	93.9(4)
O(3)-Dy(1)-N(7)	98.0(3)	N(3)-Fe(1)-N(5)	94.0(5)
O(3)-Dy(1)-N(8)	72.5(3)	N(4)-Fe(1)-N(1)	170.0(4)
O(3)-Dy(1)-N(9)	75.0(4)	N(4)-Fe(1)-N(3)	81.1(4)
O(3)-Dy(1)-N(10)	145.6(4)	N(4)-Fe(1)-N(5)	93.4(5)
O(2)-Dy(1)-O(1)	80.0(3)	N(4)-Fe(1)-N(6)	92.7(4)
O(2)-Dy(1)-O(1W)	70.2(3)	N(5)-Fe(1)-N(1)	95.5(5)
O(2)-Dy(1)-N(7)	148.9(3)	N(6)-Fe(1)-N(1)	93.1(4)
O(2)-Dy(1)-N(8)	146.5(3)	N(6)-Fe(1)-N(3)	171.6(4)
O(2)-Dy(1)-N(9)	80.2(3)	N(6)-Fe(1)-N(5)	80.7(5)
O(2)-Dy(1)-N(10)	116.8(4)		

Table S4. Selected bonds lengths [Å] and angles [°] for **3**.

3			
Dy(1)-O(1)	2.346(7)	Dy(1)-N(7)	2.705(9)
Dy(1)-O(3)	2.283(7)	Dy(1)-N(8)	2.610(9)
Dy(1)-O(2)A	2.406(7)	Dy(1)-N(9)	2.417(8)
Dy(1)-O(2)	2.445(7)	Dy(1)-N(10)	2.407(11)
Fe(1)-N(1)	1.969(8)	Fe(1)-N(4)	1.934(8)
Fe(1)-N(2)	1.906(9)	Fe(1)-N(5)	1.985(8)
Fe(1)-N(3)	1.976(9)	Fe(1)-N(6)	1.874(8)
Dy(2)-O(7)	2.346(7)	Dy(2)-N(17)	2.726(8)
Dy(2)-O(6)B	2.421(7)	Dy(2)-N(18)	2.650(9)
Dy(2)-O(6)	2.472(7)	Dy(2)-N(19)	2.382(9)
Dy(2)-O(5)	2.310(7)	Dy(2)-N(20)	2.407(10)
Fe(2)-N(11)	1.977(9)	Fe(2)-N(14)	1.940(8)
Fe(2)-N(12)	1.927(9)	Fe(2)-N(15)	1.969(9)
Fe(2)-N(13)	1.963(9)	Fe(2)-N(16)	1.915(9)
O(1)-Dy(1)-N(7)	125.5(3)	N(10)-Dy(1)-N(7)	66.4(3)
O(1)-Dy(1)-N(8)	66.4(3)	N(10)-Dy(1)-N(8)	72.8(3)
O(1)-Dy(1)-N(9)	149.9(3)	N(10)-Dy(1)-N(9)	107.0(3)
O(1)-Dy(1)-N(10)	102.6(3)	N(1)-Fe(1)-N(3)	92.2(3)
O(3)-Dy(1)-O(3)	80.2(2)	N(1)-Fe(1)-N(5)	96.8(3)
O(3)-Dy(1)-O(2)A	143.1(2)	N(2)-Fe(1)-N(1)	79.6(4)
O(3)-Dy(1)-O(2)	82.7(2)	N(2)-Fe(1)-N(3)	94.7(4)
O(3)-Dy(1)-N(7)	80.5(3)	N(2)-Fe(1)-N(4)	90.1(4)
O(3)-Dy(1)-N(8)	73.4(3)	N(2)-Fe(1)-N(5)	173.3(4)
O(3)-Dy(1)-N(9)	80.0(3)	N(3)-Fe(1)-N(5)	91.1(3)
O(3)-Dy(1)-N(10)	141.4(3)	N(4)-Fe(1)-N(1)	166.9(3)
O(2)A-Dy(1)-O(2)	60.6(3)	N(4)-Fe(1)-N(3)	80.5(3)
O(2)A-Dy(1)-N(7)	132.6(3)	N(4)-Fe(1)-N(5)	94.2(3)
O(2)-Dy(1)-N(7)	147.6(3)	N(6)-Fe(1)-N(1)	97.2(3)
O(2)A-Dy(1)-N(8)	133.2(3)	N(6)-Fe(1)-N(2)	93.8(4)
O(2)-Dy(1)-N(8)	139.6(3)	N(6)-Fe(1)-N(3)	168.3(4)
O(2)A-Dy(1)-N(9)	93.9(3)	N(6)-Fe(1)-N(4)	91.5(3)
O(2)A-Dy(1)-N(10)	75.3(3)	N(6)-Fe(1)-N(5)	81.0(4)
N(8)-Dy(1)-N(7)	59.3(3)	N(2)-O(1)-Dy(1)	119.9(6)
N(9)-Dy(1)-O(2)	77.3(3)	N(4)-O(3)-Dy(1)	120.7(6)
N(9)-Dy(1)-N(7)	72.7(3)	Dy(1)A-O(2)-Dy(1)	119.4(3)
O(7)-Dy(2)-O(6)B	88.5(2)	N(19)-Dy(2)-N(18)	124.5(3)
O(7)-Dy(2)-O(6)	79.0(2)	N(19)-Dy(2)-N(20)	107.7(3)
O(7)-Dy(2)-N(17)	125.4(2)	N(20)-Dy(2)-O(6)B	77.0(3)
O(7)-Dy(2)-N(18)	66.3(3)	N(20)-Dy(2)-O(6)	136.3(3)
O(7)-Dy(2)-N(19)	152.3(3)	N(20)-Dy(2)-N(17)	67.9(3)
O(7)-Dy(2)-N(20)	99.6(3)	N(20)-Dy(2)-N(18)	76.2(3)

O(6)B-Dy(2)-O(6)	59.3(3)	N(13)-Fe(2)-N(15)	95.3(4)
O(6)-Dy(2)-N(17)	146.5(2)	N(13)-Fe(2)-N(11)	93.9(4)
O(6)B-Dy(2)-N(17)	133.8(2)	N(14)-Fe(2)-N(13)	79.4(4)
O(6)B-Dy(2)-N(18)	139.0(2)	N(14)-Fe(2)-N(15)	171.9(4)
O(6)-Dy(2)-N(18)	137.2(3)	N(14)-Fe(2)-N(11)	93.4(4)
O(5)-Dy(2)-O(7)	84.6(2)	N(15)-Fe(2)-N(11)	93.1(4)
O(5)-Dy(2)-O(6)B	140.3(2)	N(16)-Fe(2)-N(13)	96.6(4)
O(5)-Dy(2)-O(6)	80.9(2)	N(16)-Fe(2)-N(14)	94.4(4)
O(5)-Dy(2)-N(17)	79.5(2)	N(16)-Fe(2)-N(15)	80.1(4)
O(5)-Dy(2)-N(18)	71.8(3)	N(16)-Fe(2)-N(11)	167.9(3)
O(5)-Dy(2)-N(19)	76.6(3)	N(16)-Fe(2)-N(12)	89.8(4)
O(5)-Dy(2)-N(20)	142.8(3)	N(12)-Fe(2)-N(13)	170.5(4)
N(18)-Dy(2)-N(17)	59.1(3)	N(12)-Fe(2)-N(14)	93.1(4)
N(19)-Dy(2)-O(6)B	93.0(3)	N(12)-Fe(2)-N(15)	92.8(4)
N(19)-Dy(2)-O(6)	78.0(3)	N(12)-Fe(2)-N(11)	80.6(4)
N(19)-Dy(2)-N(17)	71.2(3)		

Symmetry codes: A = -*x*+1, -*y*+1, -*z*

Table S5. Lanthanide geometry analysis by using SHAPE 2.1 program for **1**-**3**.

	SAPR-8 (D_{4d})	TDD-8 (D_{2d})	JBTPR-8 (C_{2v})	BTPR-8 (C_{2v})	JSD-8 (D_{2d})
1	0.84484	2.12733	2.18916	1.57845	4.40541
2	1.14115	1.91113	2.23563	1.62926	4.79469
3	4.62010	3.38176	2.77947	2.41491	3.01764

SAPR-8 = square antiprism; TDD-8 = triangular dodecahedron; JBTPR-8 = Biaugmented trigonal prism J50; BTPR-8 = Biaugmented trigonal prism; JSD-8 = Snub diphenoid J84.

Table S6 BVS values for Fe atoms in complexes **1**-**3**.

Complex 1			**Complex 2**		
Bond	Bond Length / Å	Bond Valence	Bond	Bond Length / Å	Bond Valence
Fe(1)-N(1)	1.965(4)	0.344	Fe(1)-N(1)	1.977(9)	0.333
Fe(1)-N(2)	1.908(4)	0.401	Fe(1)-N(2)	1.905(10)	0.404
Fe(1)-N(3)	1.972(4)	0.337	Fe(1)-N(3)	1.965(10)	0.343
Fe(1)-N(4)	1.911(4)	0.398	Fe(1)-N(4)	1.908(10)	0.401
Fe(1)-N(5)	1.970(4)	0.339	Fe(1)-N(5)	1.972(11)	0.337
Fe(1)-N(6)	1.916(4)	0.392	Fe(1)-N(6)	1.941(9)	0.366
	$\sum v$(Fe) = 2.211			$\sum v$(Fe) = 2.186	
Complex 3					
Bond	Bond Length / Å	Bond Valence	Bond	Bond Length / Å	Bond Valence
Fe(1)-N(1)	1.969(8)	0.340	Fe(2)-N(13)	1.963(9)	0.346
Fe(1)-N(2)	1.906(9)	0.403	Fe(2)-N(14)	1.940(8)	0.368
Fe(1)-N(3)	1.976(9)	0.334	Fe(2)-N(15)	1.969(9)	0.340
Fe(1)-N(4)	1.934(8)	0.373	Fe(2)-N(16)	1.915(9)	0.394
Fe(1)-N(5)	1.985(8)	0.325	Fe(2)-N(11)	1.977(9)	0.333
Fe(1)-N(6)	1.874(8)	0.440	Fe(2)-N(12)	1.927(9)	0.381
	$\sum v$(Fe) = 2.217			$\sum v$(Fe) = 2.161	

Bond Valence = $\exp[(R_0-d_{ij})/b]$, $R_0 = 1.57$, $b = 0.37$.[5]

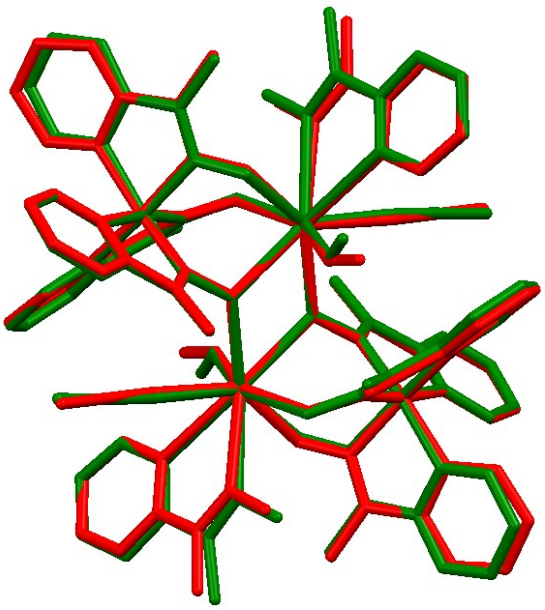

Fig. S4 Comparison of two similar asymmetric units in **3**.

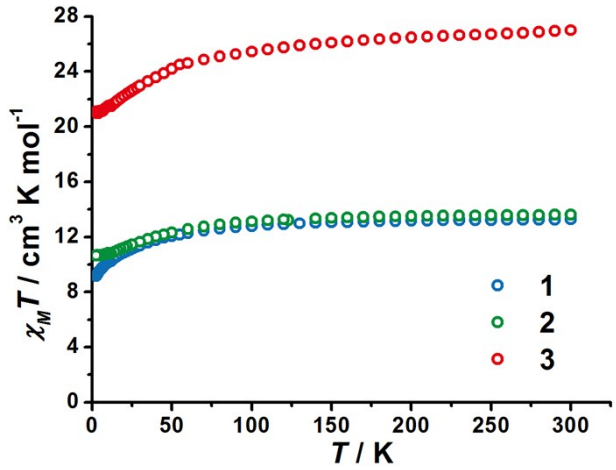

Fig. S5. Temperature dependence of the $\chi_M T$ values in 1000 Oe for **1** (blue), **2** (green) and **3** (red).

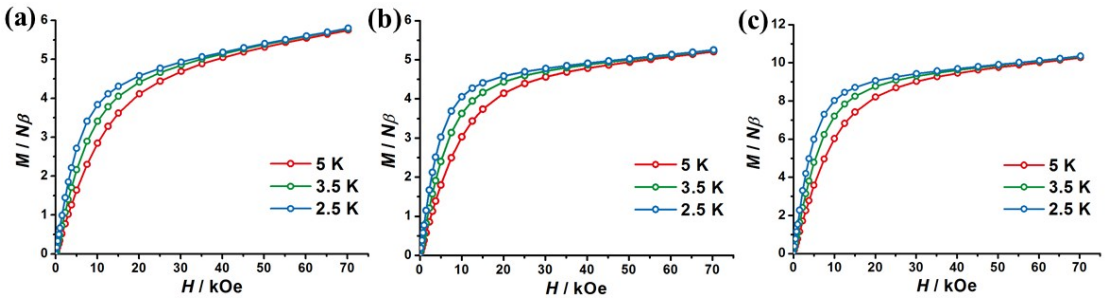

Fig. S6. Plots of *M*–*H* for **1**(a), **2**(b) and **3**(c) at 2.5, 3.5 and 5 K. The solid lines are guides to the eyes.

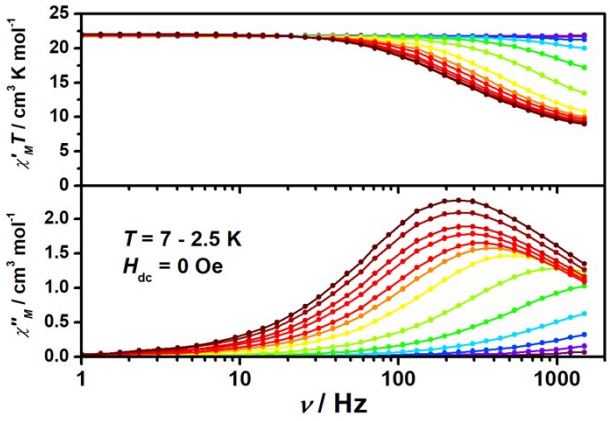

Fig. S7 Frequency dependence of the in-phase ($\chi_M'T$) and out-of-phase (χ_M'') products at zero field for **3**. The solid lines are guides to the eyes.

Table S7 Selected lanthanide complexes based on methyl-2-pyridyl ketone oxime (mepaoH) and Fe-Dy complexes.

formula	U_{eff} / K (Hdc/Oe)	ref	
$[CoDy(mepao)_3(NO_3)_3]$	16 K (600 Oe)	**6**	
$[Ni_2Dy_2(mepao)_6(NO_3)_4]$	No text	**7**	
$[ZnDy(NO_3)_2(mepko)_3(mepkoH)]$	33.3 K (1000 Oe)	**8**	
$[L_1FeDyFeL_1]ClO_4{\cdot}3CH_3OH$	No text	**9**	
$[Fe^{III}_{LS}(L_2)(\mu\text{-}L_2)Dy(NO_3)_4]$	12.9 K (1000 Oe)	**10**	
$\{[Fe^{II}_3Dy_2(L_3)_6(H_2O)_6]{\cdot}xH_2O\}_n$	No text	**11**	
$[\{Dy(hfac)_3\}_2\{Fe(L_4)_2\}]{\cdot}CHCl_3$	9.7 K	**12**	
$[Dy_4(H_2O)_8(L_5)_{14}][Fe(phen)_3]$	slow magnetic relaxation, no peak	**13**	
$[LnFe^{III}Fe^{II}_6(Hpmida)_6]{\cdot}2H_2O$	No text	**14**	
$[Fe_2Dy(L_6)_2(H_2O)]ClO_4{\cdot}2H_2O$	459 K	**15**	
$[FeDy(mepao)_3(mepaoH)(NCS)(H_2O)_2](SCN){\cdot}2H_2O$ (**1**)	no χ_M'' signal	This work	
$[FeDy(mepao)_3(mepaoH)(NCS)_2(H_2O)]{\cdot}2H_2O$ (**2**)	slow magnetic relaxation, no peak	This work	
$[Fe_2Dy_2(mepao)_6(mepaoH)_2(NCS)_4]$ (**3**)	40 (2) K	This work	

H_3L_1 = N,N',N''-tris(2-hydroxy-3-methoxybenzilidene)-2-(aminomethyl)-2-methyl-1,3-propanediamine, HL_2 = bis(2-pyridylcarbonylamine, H_2L_3 =pyridine-2,6-dicarboxylic acid, hfac =1,1,1,5,5,5-hexafluoroacetylacetonate, L_4 =bis(2-pyridylcarbonyl)amine anion, L_5 = 4-nitrobenzoato，phen = 1,10-phenanthroline H4pmida=N-(phosphonomethyl)iminodiacetic acid, H_3L_6 = 2,2',2''-(((nitrilotris(ethane-2,1-diyl))tris(azanediyl))tris(methylene)) tris(4-chlorophenol).

Ab Initio Calculations

All calculations were carried out with OpenMOLCAS[16] and are of the CASSCF/RASSI type. An entire molecule (Figure S8-S9) are included, and the coordinates of atoms are extracted from the experimentally determined crystal structure without further optimization. In complex **3**, there are two crystallographically independent Dy(III) ions, where each of the symmetric Dy(III) was replaced with a diamagnetic Y(III). The ANO-RCC basis sets have been employed as shown in Table S8.[17-20] Active space of the CASSCF method included 9 electrons in seven 4f orbitals of Dy(III). The Cholesky decomposition threshold was set to 1×10^{-8} to save disk space. All spin sextet were optimized in state-averaged calculations and then mixed by spin-orbit coupling using the restricted active space state interaction (SO-RASSI) method to obtain the *g*-tensors, energies and main magnetic axis of the ground Kramers doublet (Table S9, Figure S8-S9).[21-22]

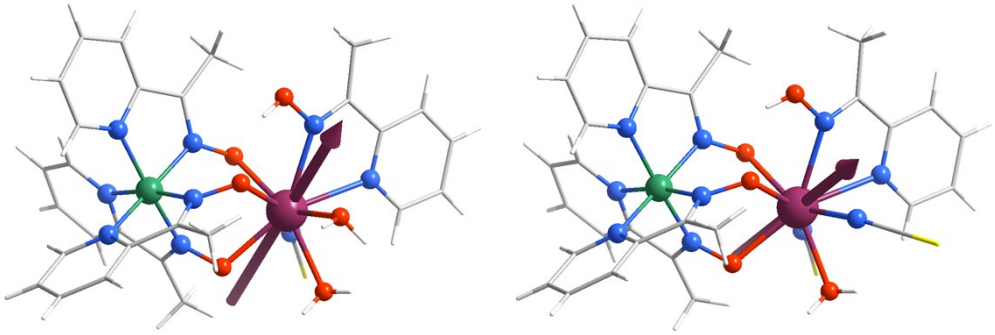

Fig. S8 The violet arrow represents the orientation of the main magnetic axis of the ground Kramers doublet obtained from the *ab initio* calculations: **1** (left), **2** (right). Color codes: Dy, violet; Fe, green; S, yellow; O, red; N, blue; C, gray; H, light gray.

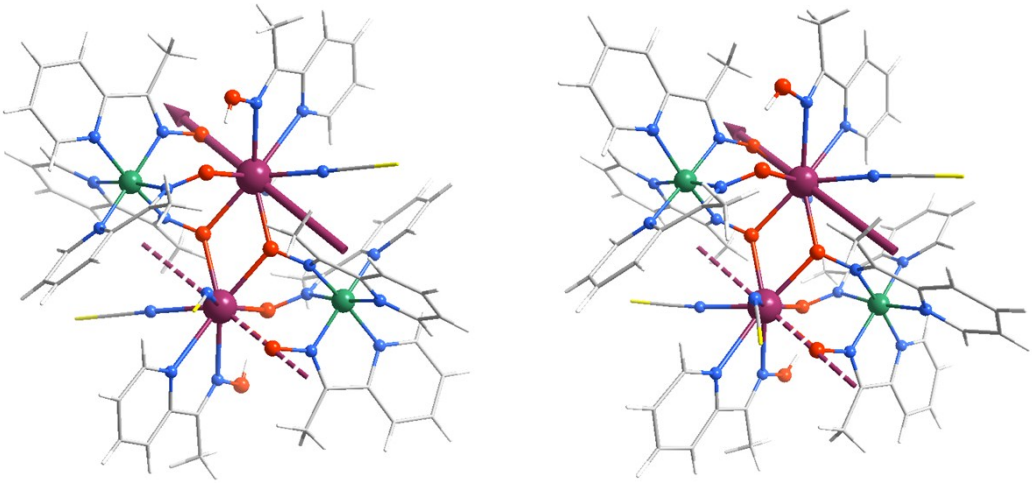

Fig. S9 The violet arrow represents the orientation of the main magnetic axis of the ground Kramers doublet obtained from the *ab initio* calculations for complex **3**: Dy1 (left), Dy2 (right). Color codes: Dy/Y, violet; Fe, green; S, yellow; O, red; N, blue; C, gray; H, light gray.

Table S8 Basis sets employed in the calculations for **1**, **2**, and **3**.

Basis set
Dy.ANO-RCC-VTZP
Y.ANO-RCC-VTZP
Fe.ANO-RCC-VTZP
O.ANO-RCC-VDZP
S.ANO-RCC-VDZP
N.ANO-RCC-VDZP
C.ANO-RCC-VDZ
H.ANO-RCC-MB

Table S9 Calculated SO-RASSI energies (in cm^{-1}) and *g*-tensors of the lowest 8 Kramers doublets for **1**, **2**, and **3**.

Complex 1				
KD	***E* / cm^{-1}**	g_X	g_Y	g_Z
1	0	1.1629	6.0810	14.5149
2	33.242	1.2137	3.0527	10.3172
3	95.208	0.4283	4.6044	11.8267
4	170.251	3.3162	5.5956	10.1234
5	250.05	0.0762	2.9021	13.0680
6	302.085	0.8862	1.3509	17.5072
7	386.081	0.3732	0.5670	19.0354
8	536.515	0.0557	0.1054	19.7551

Complex 2				
KD	***E* / cm^{-1}**	g_X	g_Y	g_Z
1	0	0.4137	0.7563	18.9053
2	27.216	0.2987	1.0880	16.1103
3	70.394	1.1890	2.5882	13.0788
4	125.866	1.8476	5.1729	9.8007
5	178.343	9.7519	6.4171	2.6570
6	245.791	1.5094	2.3508	14.8816
7	324.488	0.5532	1.1100	18.7819
8	488.839	0.0275	0.0618	19.7312

Complex 3 (Dy1)				
KD	***E* / cm^{-1}**	g_X	g_Y	g_Z
1	0	0.0345	0.0606	19.8038
2	127.313	1.9670	6.3599	12.5827
3	168.111	7.9474	5.0913	1.8274
4	200.376	0.0520	0.9318	15.5301
5	262.643	2.3845	2.8428	10.4306
6	314.844	0.3653	1.7683	13.1182

7	327.412	0.8444	1.7920	15.3115
8	386.052	0.3594	0.9011	17.1908

Complex 3 (Dy2)				
KD	***E* / cm^{-1}**	g_X	g_Y	g_Z
1	0	0.1084	0.1870	19.5917
2	102.616	1.7122	4.7357	11.3407
3	115.918	1.0470	2.3925	15.5842
4	153.891	6.6875	5.1864	1.1838
5	219.461	0.3405	2.4366	12.9794
6	257.985	0.8626	3.9926	11.6647
7	293.441	1.8965	5.2145	10.2391
8	347.858	0.2981	0.7193	18.0550

Reference

1. P. Chaudhuri, T. Weyhermüller, R. Wagner, S. Khanra, B. Biswas, E. Bothe and E. Bill, *Inorg. Chem.*, 2007, **46**, 9003-9016.
2. O. V. Dolomanov, L. J. Bourhis, R. J. Gildea, J. A. Howard and H. Puschmann, *J. Appl. Crystallogr.*, 2009, **42**, 339-341.
3. G. M. Sheldrick, *Acta Crystallographica Section C: Structural Chemistry*, 2015, **71**, 3-8.
4. A. L. Spek, *J. Appl. Crystallogr.*, 2003, **36**, 7–13.
5. H. Zheng, K. M. Langner, G. P. Shields, J. Hou, M. Kowiel, F. H. Allen, G. Murshudov and W. Minor, *Acta crystallographica. Section D, Structural biology*, 2017, **73**, 316-325.
6. C. D. Polyzou, E. S. Koumousi, Z. G. Lada, C. P. Raptopoulou, V. Psycharis, M. Rouzières, A. C. Tsipis, C. Mathonière, R. Clérac and S. P. Perlepes, *Dalton Transactions*, 2017, **46**, 14812-14825.
7. C. Papatriantafyllopoulou, M. Estrader, C. G. Efthymiou, D. Dermitzaki, K. Gkotsis, A. Terzis, C. Diaz and S. P. Perlepes, *Polyhedron*, 2009, **28**, 1652-1655.
8. N. C. Anastasiadis, C. D. Polyzou, G. E. Kostakis, V. Bekiari, Y. Lan, S. P. Perlepes, K. F. Konidaris and A. K. Powell, *Dalton Trans.*, 2015, **44**, 19791-19795.
9. T. Yamaguchi, J.-P. Costes, Y. Kishima, M. Kojima, Y. Sunatsuki, N. Bréfuel, J.-P. Tuchagues, L. Vendier and W. Wernsdorfer, *Inorg. Chem.*, 2010, **49**, 9125-9135.
10. M. Ferbinteanu, T. Kajiwara, K.-Y. Choi, H. Nojiri, A. Nakamoto, N. Kojima, F. Cimpoesu, Y. Fujimura, S. Takaishi and M. Yamashita, *J. Am. Chem. Soc.*, 2006, **128**, 9008-9009.
11. X.-Q. Zhao, P. Cui, B. Zhao, W. Shi and P. Cheng, *Dalton Transactions*, 2011, **40**, 805-819.
12. F. Pointillart, K. Bernot, R. Sessoli and D. Gatteschi, *Chem. Eur. J.*, 2007, **13**, 1602-1609.
13. Y. Zhu, F. Luo, Y.-m. Song, H.-x. Huang, G.-m. Sun, X.-z. Tian, Z.-Z. Yuan, Z.-w. Liao, M.-b. Luo, S.-j. Liu, W.-y. Xu and X.-F. Feng, *Dalton Trans.*, 2012, **41**, 6749-6755.
14. T.-H. Yang, A. R. Silva, L. Fu and F.-N. Shi, *Dalton Trans.*, 2015, **44**, 13745-13751.
15. J.-L. Liu, J.-Y. Wu, Y.-C. Chen, V. Mereacre, A. K. Powell, L. Ungur, L. F. Chibotaru, X.-M. Chen and M.-L. Tong, *Angew. Chem. Int. Ed.*, 2014, **53**, 12966-12970.
16 A. Francesco, A. Jochen, C. R. K., C. L. F., D. M. G., D. V. Luca, F. G. Ignacio, F. Nicolas, F. L. Manuel, G. Laura, G. Marco, G. Angelo, H. C. E., L. M. Giovanni, L. Hans, M. Dongxia, M. P. Åke, M. Thomas, N. Artur, O. Massimo, P. T. Bondo, P. Daoling, P. Felix, P. Ben, R. Markus, R. Ivan, S. Igor, S.-M. Javier, S. Michael, T. D. G., U. Liviu, V. Alessio, V. Steven, V. Valera, V. V. P., W. Oliver, Z. Felipe and L. Roland, *J. Comput. Chem.*, 2016, **37**, 506-541.
17 B. O. Roos, R. Lindh, P.-Å. Malmqvist, V. Veryazov, P.-O. Widmark and A. C. Borin, *J. Phys. Chem. A*, 2008, **112**, 11431-11435.
18 B. O. Roos, R. Lindh, P.-Å. Malmqvist, V. Veryazov, P.-O. Widmark, *J. Phys. Chem. A*, 2005, **109**, 6575-6579.
19 B. O. Roos, R. Lindh, P.-Å. Malmqvist, V. Veryazov and P.-O. Widmark, *J. Phys. Chem. A*, 2004, **108**, 2851-2858.
20 P.-O. Widmark, P. Å. Malmqvis, B. O. Roos, *Theor. Chim. Acta* 1990, **77**, 291-306.
21 P. Å. Malmqvist, B. O. Roos and B. Schimmelpfennig, *Chem. Phys. Lett.*, 2002, **357**, 230-240.
22 L. F. Chibotaru, L. Ungur, *J. Chem. Phys.* 2012, **137**, 064112.